



RESEARCH PAPER

***MdHB1* down-regulation activates anthocyanin biosynthesis in the white-fleshed apple cultivar ‘Granny Smith’**

Yonghua Jiang^{*}, Cuihua Liu^{*}, Dan Yan, Xiaohong Wen, Yanli Liu, Haojie Wang, Jieyu Dai, Yujie Zhang, Yanfei Liu, Bin Zhou and Xiaolin Ren[†]

College of Horticulture, Northwest A&F University, Yangling, Shaanxi 712100, China

^{*} These authors contributed equally to this work.

[†] Correspondence: renxl@nwfau.edu.cn

Received 3 November 2016; Editorial decision 9 January 2017; Accepted 9 January 2017

Editor: Robert Hancock, The James Hutton Institute

Abstract

Coloration in apple (*Malus domestica*) flesh is mainly caused by the accumulation of anthocyanin. Anthocyanin is biosynthesized through the flavonoid pathway and regulated by MYB, bHLH, and WD40 transcription factors (TFs). Here, we report that the HD-Zip I TF *MdHB1* was also involved in the regulation of anthocyanin accumulation. *MdHB1* silencing caused the accumulation of anthocyanin in ‘Granny Smith’ flesh, whereas its overexpression reduced the flesh content of anthocyanin in ‘Ballerina’ (red-fleshed apple). Moreover, flowers of transgenic tobacco (*Nicotiana tabacum* ‘NC89’) overexpressing *MdHB1* showed a remarkable reduction in pigmentation. Transient promoter activation assays and yeast one-hybrid results indicated that *MdHB1* indirectly inhibited expression of the anthocyanin biosynthetic genes encoding dihydroflavonol-4-reductase (*DFR*) and UDP-glucose:flavonoid 3-O-glycosyltransferase (*UFGT*). Yeast two-hybrid and bimolecular fluorescence complementation determined that *MdHB1* acted as a homodimer and could interact with MYB, bHLH, and WD40 in the cytoplasm, consistent with its cytoplasmic localization by green fluorescent protein fluorescence observations. Together, these results suggest that *MdHB1* constrains *MdMYB10*, *MdbHLH3*, and *MdTTG1* to the cytoplasm, and then represses the transcription of *MdDFR* and *MdUFGT* indirectly. When *MdHB1* is silenced, these TFs are released to activate the expression of *MdDFR* and *MdUFGT* and also anthocyanin biosynthesis, resulting in red flesh in ‘Granny Smith’.

Key words: Anthocyanin biosynthesis, ‘Granny Smith’, homeobox, *MdHB1*, *MdMYB10*, red-fleshed apple, subcellular localization, virus-induced gene silencing.

Introduction

As a popular fresh fruit, apple (*Malus domestica*) is rich in flavonoids (Balázs *et al.*, 2012; Bondonno *et al.*, 2012), which are secondary metabolites contributing to plant environmental adaptation (Kovinich *et al.*, 2014), fruit development (Petroni and Tonelli, 2011; Jaakola, 2013), and human health (Alipour *et al.*, 2016). Given their remarkable levels of health-benefitting flavonoids, red-fleshed apples of good quality are desirable for breeding (Sun-Waterhouse *et al.*, 2013; Faramarzi *et al.*, 2014, 2015; Wang *et al.*, 2015).

Among the flavonoids, anthocyanins cause the red color in apple peel and flesh (Tako *et al.*, 2006a; Espley *et al.*, 2007; Chagné *et al.*, 2013; Zhang *et al.*, 2013; Wang *et al.*, 2015). Anthocyanins are synthesized via the flavonoid pathway, which has branches for the synthesis of flavonols and proanthocyanidins (Fig. 1) (Tako *et al.*, 2006b). The mRNA abundances of most structural genes, such as those encoding chalcone synthase (*CHS*), flavanone 3-hydroxylase (*F3H*), dihydroflavonol-4-reductase (*DFR*), and

UDP-glucose:flavonoid 3-*O*-glycosyltransferase (*UFGT*), are highly correlated with the accumulation of anthocyanin (Boss *et al.*, 1996; Takos *et al.*, 2006a; Lou *et al.*, 2014). Some transcription factors (TFs; e.g. MYB, bHLH, and WD40) are also involved in the regulation of anthocyanin intensity and accumulation pattern (Albert *et al.*, 2011; An *et al.*, 2012; Schaart *et al.*, 2013; Li *et al.*, 2014; Xu *et al.*, 2014; Montefiori *et al.*, 2015). MYB, bHLH, and WD40 TFs usually form MYB-bHLH-WD40 (MBW) complexes to regulate the so-called late biosynthetic genes, such as *DFR*, anthocyanidin reductase (*ANR/BAN*), and anthocyanidin synthase (*ANS*), but have little or no effect on the early biosynthetic genes (Baudry *et al.*, 2006; Gonzalez *et al.*, 2008; Xu *et al.*, 2014).

MYB TFs are believed to be the key components in MBW complexes (Jaakola, 2013). DEEP PURPLE and PURPLE HAZE are R2R3 MYBs in petunia (*Petunia hybrida*), controlling anthocyanin production in vegetative tissues and promoting floral pigmentation (Aharoni *et al.*, 2011); in contrast, PhMYBx (R3-MYB) and PhMYB27 (R2R3-MYB) are two repressors, which participate in hierarchical and feedback regulation with other MYBs or TFs in the MBW complex to respond to developmental and environmental changes (Albert *et al.*, 2014). In apple, it has been described that the R2R3 MYB TFs MYBA and MYB1 positively regulate fruit peel color (Takos *et al.*, 2006a; Ban *et al.*, 2007), while their allelic protein MYB10 is considered to control the red pigmentation in flesh (Espley *et al.*, 2007). MYB10a, a paralog of MYB10, is also implicated in the red-fleshed phenotype (Chagne *et al.*, 2013). In addition, white- and red-fleshed apples carry the same MYB10 protein, but structural differences in their

promoters lead to different transcript levels and flesh traits (Espley *et al.*, 2009).

Although study of the transcriptional control of anthocyanin has mainly focused on diverse MBW complexes (Petroni and Tonelli, 2011; Xu *et al.*, 2014; Montefiori *et al.*, 2015), other TFs are also considered to be involved in the regulation of anthocyanin accumulation, such as NAC TFs in peach (*Prunus persica*) (Zhou *et al.*, 2015) and SVP3 in kiwifruit (*Actinidia* spp.) (Wu *et al.*, 2014). Here, we report a homeodomain-leucine zipper (HD-Zip) I protein MdHb1 in apple, which is also associated with anthocyanin pigmentation.

HD-Zip protein is composed of a homeobox domain (HD), acting as a DNA-binding site, and a homeobox domain-associated leucine zipper (Zip), which promotes DNA binding and homo- or heterodimerization (Sessa *et al.*, 1993; Papadopoulos *et al.*, 2012). Previous studies have shown that HD-Zip I subfamily genes are involved in environmental stress responses (Matsumoto *et al.*, 2014; Kovalchuk *et al.*, 2016; Romani *et al.*, 2016; Song *et al.*, 2016), fruit ripening (Lin *et al.*, 2008), and flower senescence (Lu *et al.*, 2014). However, only a few studies have focused on their roles in anthocyanin accumulation. *ANTHOCYANINLESS2* (here named *AtANL2*) is the first HD-Zip IV gene revealed to be involved in the tissue-specific accumulation of anthocyanin (Kubo *et al.*, 1999), but its expression was not significantly affected by irradiation and *TTG1* defects, which influence anthocyanin content in *Arabidopsis thaliana* (Kubo *et al.*, 2008). Recently, several other HD-Zip TFs have been suggested to influence the accumulation of anthocyanin (Zhang *et al.*, 2010; Lu *et al.*, 2014; Sun *et al.*, 2015). However, the regulatory function of HD-Zip TFs in anthocyanin pigmentation still remains unclear.

In this study, we propose that MdHb1 represses the accumulation of anthocyanin in apple flesh, which was proved by virus-induced gene silencing (VIGS) and transient overexpression assays in some white- and red-fleshed apples, respectively. The molecular events underlying this are discussed, especially the regulation of the anthocyanin biosynthetic genes *MdDFR* and *MdUFGT* by MdHb1 and MdMYB10. Our study not only enhances our functional understanding of HD-Zip TFs, but also provides a deeper understanding of the control of anthocyanin biosynthesis.

Materials and methods

Plant materials

White-fleshed apple fruit ‘Granny Smith’ were collected at 25, 40, 70, 100, and 120 d after full bloom from the orchard of the Northwest A&F University apple experimental station in Guancun, Shaanxi, China, in 2014. Flesh samples were prepared. Leaves and flower buds were picked in April 2014. ‘Ballerina’ was maintained in the orchard of the Northwest A&F University apple experimental station in Qianyang, Shaanxi, China. Mature fruit were collected in September 2015. For treated fruit, flesh samples were prepared from the injection areas (indicated in the relevant figures). Samples were analyzed immediately or frozen in liquid nitrogen for further analyses.

For *Agrobacterium tumefaciens*-mediated infiltration, *Nicotiana tabacum* ‘NC89’ and *N. benthamiana* seeds were cultivated in a light

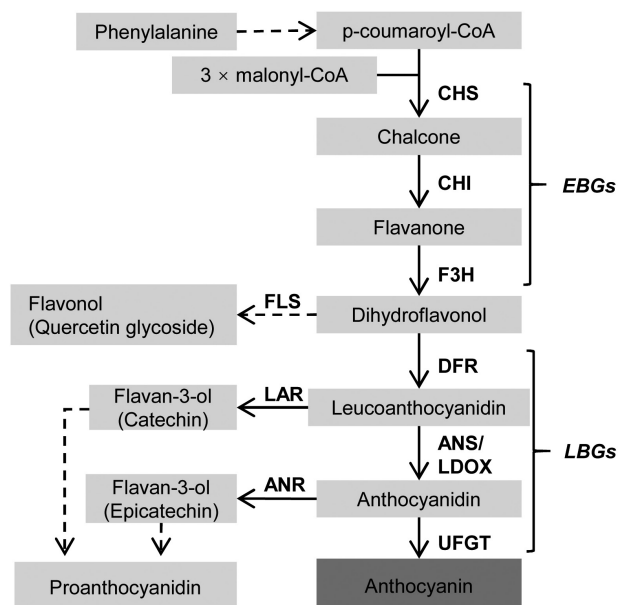


Fig. 1. Diagrammatic representation of the flavonoid pathway leading to synthesis of anthocyanin, flavonol, and proanthocyanidin in apple (*Malus domestica*). Abbreviated enzyme names are shown as follows: CHS, chalcone synthase; CHI, chalcone isomerase; F3H, flavanone 3-hydroxylase; DFR, dihydroflavonol-4-reductase; ANS, anthocyanidin synthase; UFGT, UDP-glucose:flavonoid 3-*O*-glycosyltransferase; FLS, flavonol synthase; LAR, leucoanthocyanidin reductase; ANR, anthocyanidin reductase. EBGs, early biosynthetic genes; LBGs, late biosynthetic genes.

growth chamber (16 h light/8 h dark, 22 °C/18 °C). The light intensity was 200 $\mu\text{mol m}^{-2} \text{s}^{-1}$. Light growth chambers in this study were all regulated under the same conditions.

Quantitative reverse transcription-PCR (RT-PCR)

Total RNA was extracted using the SDS-phenol method (Hu *et al.*, 2002). The RNA concentration and quality were detected by running on a 1.0% agar ethidium bromide-stained gel. A 1 mg aliquot of total RNA was reverse-transcribed to cDNA using the PrimeScript RT reagent kit with gDNA Eraser (TaKaRa, Dalian, China). Quantitative RT-PCR was performed on an Icyler iQ5 (Bio-Rad, Berkeley, CA, USA) with the SYBR Premix Ex Taq II (TaKaRa), in accordance with the manufacturer's instructions. Target gene expression was normalized to that of the internal reference gene (*Actin*) using the $2^{-\Delta\Delta\text{CT}}$ method. All reactions were run in three replicates for each biological repeat. All primers used in this study are listed in Supplementary Table S1 at JXB online.

Subcellular localization experiments

The full coding sequence of *MdHBI* was PCR-amplified from the flower cDNA of 'Granny Smith'. *MdHBI*, with a C-terminal green fluorescent protein (GFP) tag, was inserted into the plant binary expression vector pVBG2307 (Ahmed *et al.*, 2012), under the control of the *Cauliflower mosaic virus* 35S promoter (35S), to form 35S:*MdHBI*-GFP. Vectors in which only the *GFP* gene was inserted were used as a positive control (35S:*GFP*). ProHB (promoter of *MdHBI*; Supplementary Fig. S1) was cloned from genomic DNA of 'Granny Smith' to construct the ProHB:*GFP* plasmid by replacing 35S. Plasmids were transformed into *Agrobacterium tumefaciens* strain GV3101(pMP90) through electroporation.

For transient expression, the *A. tumefaciens* strains were kept at 28 °C in LB medium with appropriate antibiotics and then resuspended in infiltration buffer (10 mM MgCl_2 , 10 mM MES, 150 μM acetosyringone) to a final OD_{600} of 0.5. Approximately 200 μl of *A. tumefaciens* solution was infiltrated at one point into a young leaf of 'NC89' with a 1 ml needleless syringe. Plants were placed under shaded conditions at room temperature for 72 h, and then GFP fluorescence was observed with a Leica AF6000 microscope (Leica Microsystems, Wetzlar, Germany). All transient expression assays were repeated four times with similar results.

RNAi transient tests in white-fleshed 'Granny Smith' using the VIGS system

Fragments specific to *MdHBI* or *MdMYB10* were amplified from the flower cDNA of 'Granny Smith'. The products were sequenced and cloned into pTRV2 to form pTRV2-*MdHBI*s/pTRV2-*MdMYB10*. The vectors were transformed into *A. tumefaciens* strain GV3101(pMP90) for the VIGS experiment, as described previously (Lin *et al.*, 2008). Briefly, *A. tumefaciens* strains carrying the VIGS constructs were incubated, harvested, and resuspended in the infiltration buffer to a final OD_{600} of 0.8. *Agrobacterium tumefaciens* strains containing pTRV1 were mixed with strains harboring pTRV2 or its derivatives, and incubated at room temperature without shaking for 2 h before infiltration.

For the first sampling time, 'Granny Smith' fruit at commercial maturity were obtained in September 2014. A total of 80 fruit were selected and randomly divided into two groups, namely 40 control fruit (named pTRV2; pTRV1:pTRV2=1:1, v/v) and 40 pTRV2-*MdHBI*-treated fruit (pTRV1:pTRV2-*MdHBI*=1:1, v/v). For fruit infiltration, four points evenly spaced around the middle of the fruit were selected and each point was injected with 300 μl of an *A. tumefaciens* mixture using a 1 ml syringe. The needle was injected vertically. After treatments, fruit were air-dried, packed in PVC bags with ventilation holes, and stored in a light growth chamber. After treatment for 1, 3, 5, and 7 d, flesh tissues inside the injection areas of 10 fruit were prepared. Each time point contained four independent

biological replicates and each replicate contained flesh tissues from two or three fruit, depending on the silencing effects.

For the second sampling time, 'Granny Smith' fruit were picked in September 2015. Forty fruit were selected and randomly divided into four groups, namely 10 control fruit, 10 pTRV2-*MdHBI*-, 10 pTRV2-*MdMYB10*- (pTRV1:pTRV2-*MdMYB10*=1:1, v/v), and 10 pTRV2-*MdHBI*+pTRV2-*MdMYB10*-treated fruit (pTRV1:pTRV2-*MdHBI*:pTRV2-*MdMYB10*=2:1:1, v/v/v). The needle was injected at an angle of 45°. Fruit were placed in a light growth chamber. Flesh tissues were photographed and sampled after treatment for 5 d.

Transient overexpression assays in red-fleshed 'Ballerina'

The full-length *MdHBI* was introduced into pVBG2307, under the control of 35S, to form 35S:*MdHBI*. The *A. tumefaciens*-mediated plant infiltration was carried out as described for VIGS. Ten mature 'Ballerina' fruit were selected for the transient overexpression of *MdHBI*, while another 10 fruit infiltrated with empty pVBG2307 vectors were chosen as a control. After treatments, all of the fruit were placed in a light growth chamber for 5 d. For each treatment, three biological replicates were prepared.

Agrobacterium tumefaciens-mediated genetic transformation of *MdHBI* into 'NC89'

The 35S:*MdHBI* plasmids were also used for the stable transformation in 'NC89' by *A. tumefaciens*-mediated transformation (Sunilkumar *et al.*, 1999). Tobacco plants were grown in a light growth chamber. Flowers in full bloom were sampled for subsequent experiments.

Anthocyanin measurements

For 'Granny Smith', 0.5 g of flesh tissue was ground and then extracted in 1% (v/v) HCl-methanol for 24 h at 4 °C in the dark. After centrifugation, the upper aqueous phase was injected into an HP1200 Liquid Chromatograph (Agilent Technology, Palo Alto, CA, USA) for HPLC analysis. Data at 280, 320, and 520 nm were collected and analyzed as described previously (Chen *et al.*, 2012).

For 'Ballerina' and 'NC89', the total anthocyanin content was measured using the pH differential method (Wolfe and Liu, 2003). The absorbance values in 25 mM potassium chloride buffer (pH 1.0) and 0.4 M sodium acetate buffer (pH 4.5) were measured simultaneously at 515 nm and 700 nm using a UV-visible spectrophotometer (UV-2450; Shimadzu, Kyoto, Japan). The relative anthocyanin content was expressed as mg kg^{-1} FW.

Transient dual-luciferase detection and CCD imaging

The promoter sequences of *MdMYB10*, *MdUFGT*, and *MdDFR* (named ProMYB, ProUFGT, and ProDFR, respectively) were cloned from genomic DNA of 'Granny Smith' (Supplementary Fig. S1). The full-length coding sequences of *MdTTG1*, *MdbHLH3*, and *MdMYB10* were amplified from flower cDNA of 'Granny Smith'. ProUFGT/ProDFR was cloned into pGreenII 0800-LUC vector to fuse with the luciferase (LUC) reporter gene (ProUFGT/ProDFR-LUC), while *MdbHLH3*, *MdHBI*, *MdMYB10*, and *MdTTG1* effectors were cloned into pGreenII 62-SK vectors. *Agrobacterium tumefaciens* strains containing TF plasmids were mixed with those strains harboring promoter plasmids at a volume ratio of 9:1. The mixtures were incubated at room temperature without shaking for 2 h, before they were infiltrated into *N. benthamiana* leaves (Hellens *et al.*, 2005).

Firefly LUC and *Renilla* LUC activities were assayed using dual-luciferase assay reagents (Beyotime, Nanjing, China). After treatment for 3 d, 1 cm leaf discs around the injection sites (six technical replicates) were removed and ground in 500 μl of passive lysis buffer. Subsequently, 10 μl of a 1/100 dilution of this crude extract was

assayed in 90 μ l of LUC assay buffer, and the resultant chemiluminescence was measured (Luc). *Renilla* LUC test buffer (100 μ l) was added, and a second chemiluminescence measurement was recorded (Ren). Absolute relative luminescence units were measured using a multifunctional microplate reader, Tecan Infinite M200 Pro (TECAN, Hombrechtikon, Switzerland), with a 5 s delay and 15 s integrated measurements. Measurements were repeated four times with similar results.

Imaging of the LUC reporter requires application of the exogenous substrate luciferin. The leaf discs were sprayed uniformly five times with 1 mM luciferin (Promega, Madison, WI, USA) in 0.01% Triton X-100 water solution. The discs were kept in the dark for 5 min to quench the background fluorescence. A low-light cooled CCD imaging apparatus (Lumazone Pylon 2048B; Roper Industries, Trenton, NJ, USA) and Winview imaging software were used to capture the LUC images. The exposure time was 8 min.

Analyses of β -glucuronidase (GUS) activities

To construct another set of reporter plasmids, ProUFGT, ProDFR, ProHB, and ProMYB were cloned into pC0390GUS vectors (promoter–GUS). The effector plasmids were the same as those used in the dual-luciferase assay. *Agrobacterium tumefaciens* strains containing reporter plasmids were mixed equally (v/v) with those strains harboring effector plasmids. After incubation, the mixtures were injected into ‘NC89’ leaves.

The histochemical detection of GUS activity was performed as described previously (Yu *et al.*, 2013). The resultant fluorescence was measured using an Infinite M200 Pro (TECAN) at an excitation wavelength of 365 nm and an emission wavelength of 455 nm. GUS activity was expressed as picomolar of 4-methylumbelliferone (4-MU; Sigma-Aldrich, Shanghai, China) generated per second per kg of soluble protein. The GUS measurements were repeated four times with similar results.

Yeast one-hybrid (Y1H)

The Y1H assays were performed following the manufacturer’s instructions for the Matchmaker Gold Yeast One-Hybrid System Kit (Clontech, Mountain View, CA, USA). ProUFGT and ProDFR were individually ligated into pAbAi to construct the pAbAi-baits. *MdHBI* and *MdMYB10* were separately inserted into pGADT7 to construct the AD-prey vectors. The pAbAi-baits were linearized and transformed into Y1HGold separately, and selected in a plate with selective synthetic dextrose medium (SD) lacking uracil. Colony PCR analysis (Matchmaker Insert Check PCR Mix 1; Clontech) was used to confirm that the plasmids had integrated correctly into the genome of Y1HGold. After determining the minimal inhibitory concentration of Aureobasidin A (AbA) for the bait yeast strains, the AD-prey vectors were transformed into the bait yeast strains and screened on an SD/-Leu/AbA plate. All transformations and screenings were performed three times.

Yeast two-hybrid (Y2H)

Y2H was performed using the Matchmaker™ GAL4 yeast two-hybrid system (Clontech). The truncated *MdHBI* Δ (Supplementary Fig. S2) was inserted into pGBKT7 to generate the bait plasmid BD-*MdHBI* Δ . The bait vectors were transformed into the Y2HGold yeast strain and screened on an SD/-Trp/X- α -gal plate. At the same time, the coding sequences of *MdTTG1* and *MdbHLH3* were individually cloned into pGADT7 to form AD-prey vectors. The four AD-prey vectors (another two vectors constructed in Y1H) were separately transformed into the BD-*MdHBI* Δ -containing Y2HGold yeast strain and plated on SD/-Trp/-Leu/-His/-Ade/X- α -gal for photographing.

Bimolecular fluorescence complementation (BiFC)

The full-length *MdHBI* was cloned into pSPYCE(M) to generate *MdHBI*CE, and the full coding sequences of *MdHBI*,

MdMYB10, *MdTTG1*, and *MdbHLH3* were individually cloned into pSPYNE(R)173 (named *MdHBI*NE, *MdMYB10*NE, *MdTTG1*NE, and *MdbHLH3*NE). *Agrobacterium tumefaciens* strains containing *MdHBI*CE plasmid were mixed equally (v/v) with strains harboring NE series plasmids (Yu *et al.*, 2013). The following transient expression in *N. benthamiana* and the observation of yellow fluorescent protein (YFP) fluorescence were conducted as described in the subcellular localization section.

Results

MdHBI encodes an HD-Zip I protein

The HD-Zip protein *LeHBI* has been reported to be involved in fruit ripening of tomato (*Solanum lycopersicum*) (Lin *et al.*, 2008). A BLAST search using the *LeHBI* cDNA sequence was performed in the Genome Database for Rosaceae (<https://www.rosaceae.org/>). The complete coding sequence of *MdHBI* was identified and cloned from ‘Granny Smith’ flowers. This *MdHBI* encodes a protein of 336 amino acids with a conserved HD (amino acids 77–133) and Zip (amino acids 134–178) (Supplementary Fig. S2). *MdHBI* sequences from ‘Granny Smith’ and ‘Royal Gala’ show high conservation and differ from each other by only two amino acids (34 and 38). Sequence alignment suggests that our *MdHBI* belonging to the HD-Zip I TF family is most similar to *LeHBI* among the selected sequences (Fig. 2A). Its HD-Zip domain shares 84% and 86% similarity to those of *AtHBI* and *LeHBI*, respectively (Fig. 2B).

Subcellular localization and expression profiling of *MdHBI*

MdHBI was predicted to be located in the nucleus (certainty=0.600) and the microbody (certainty=0.407) by PSORT (<http://psort.hgc.jp/form.html>). To determine the accuracy of this, localization analyses were performed by transient assays in ‘NC89’ leaves. The results showed that the GFP fluorescence of 35S:*MdHBI*–GFP was diffuse in the cytoplasm and was concentrated in the nucleus, similar to the case of 35S:GFP, which acted as a positive control (Fig. 3A). In contrast, the fluorescence of ProHB:GFP was detected only in the cytoplasm. It was difficult to observe the ProHB:GFP signal in the nucleus during our four independent experiments.

Next, the *MdHBI* expression profile in various organs was measured using quantitative RT–PCR. As shown in Fig. 3B, *MdHBI* was highly expressed in flower buds and young leaves compared with flesh tissues. During fruit developmental stages, *MdHBI* expression levels in flesh exhibited a ‘V’-type distribution, with higher levels at stages 3 and 7, when fruit were young and commercially mature, respectively.

Virus-induced *MdHBI* silencing leads to a red coloration in ‘Granny Smith’ flesh

To explore the potential role of *MdHBI*, three *MdHBI*-specific fragments were designed for VIGS experiments in ‘Granny Smith’ fruit at stage 7. After 3 d, there was red staining in flesh around the injection holes, but no coloration was

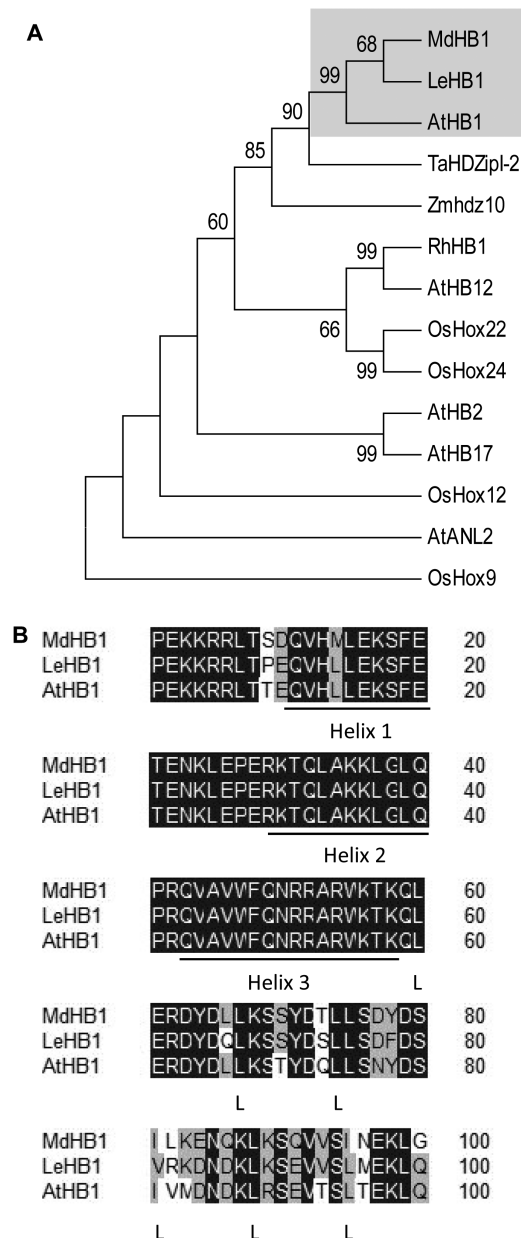


Fig. 2. Sequence analysis of MdHB1. (A) Phylogenetic tree of the selected HD-Zip proteins. The phylogenetic tree was constructed with MEGA version 6.06 using the Neighbor-Joining method and 1000 bootstrap replicates. GenBank accession numbers for HD-Zip proteins are given in Supplementary Data S1. (B) Comparison of MdHB1 HD-Zip amino acid sequences with those from Arabidopsis AtHB1 and tomato LeHB1. The three α -helices of the homeodomain and the leucine (or valine) residues are identified.

observed in peel (similar to the trait on day 5 in Fig. 4A). For the control (pTRV2), neither flesh nor peel presented any coloration. Further analyses showed that all the fragments exhibited decreased expression levels of *MdHB1* relative to pTRV2, and Fragment 1 was most effective at achieving this (Supplementary Fig. S3). Thus, Fragment 1 was selected for the following VIGS tests. Because the application of VIGS in young fruit (stage 3) displayed no clear phenotype, the roles of MdHB1 were explored with mature fruit (stage 7). Semi-quantitative RT-PCR with fruit treated for 5 d showed that

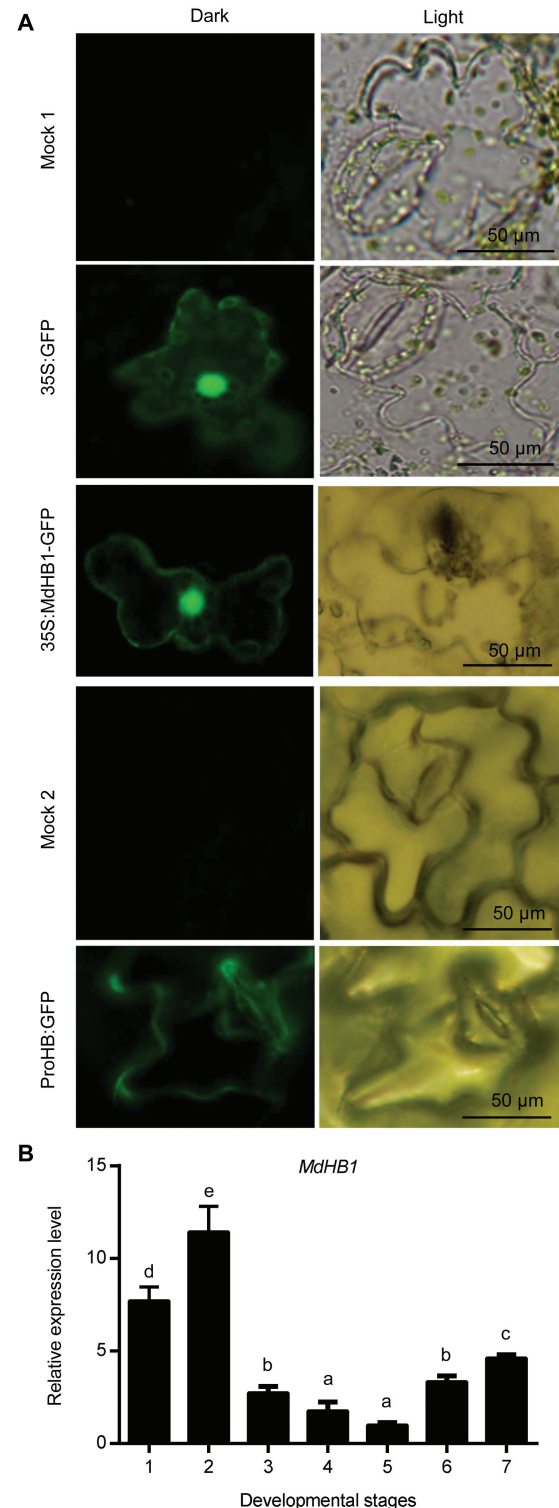


Fig. 3. Normal characters of *MdHB1*. (A) Subcellular localization of MdHB1 in *Nicotiana tabacum* 'NC89' leaves. Experiments were repeated four times. Mocks, untreated leaves. Images in the top three lines are the results observed with the lower epidermal cells. The bottom two lines show the observations of the entire small pieces of leaves. ProHB, *MdHB1* promoter. (B) Quantitative reverse transcription-PCR (RT-PCR) analysis of *MdHB1* expression in different tissues of 'Granny Smith'. Stage 1, leaves; stage 2, flower buds. Stages 3–7 are flesh samples of fruit collected at 25, 40, 70, 100, and 120 d after full bloom. Values are means \pm SD, $n=3$. Different letters denote statistical significance (one-way ANOVA, $P<0.05$). (This figure is available in colour at JXB online.)

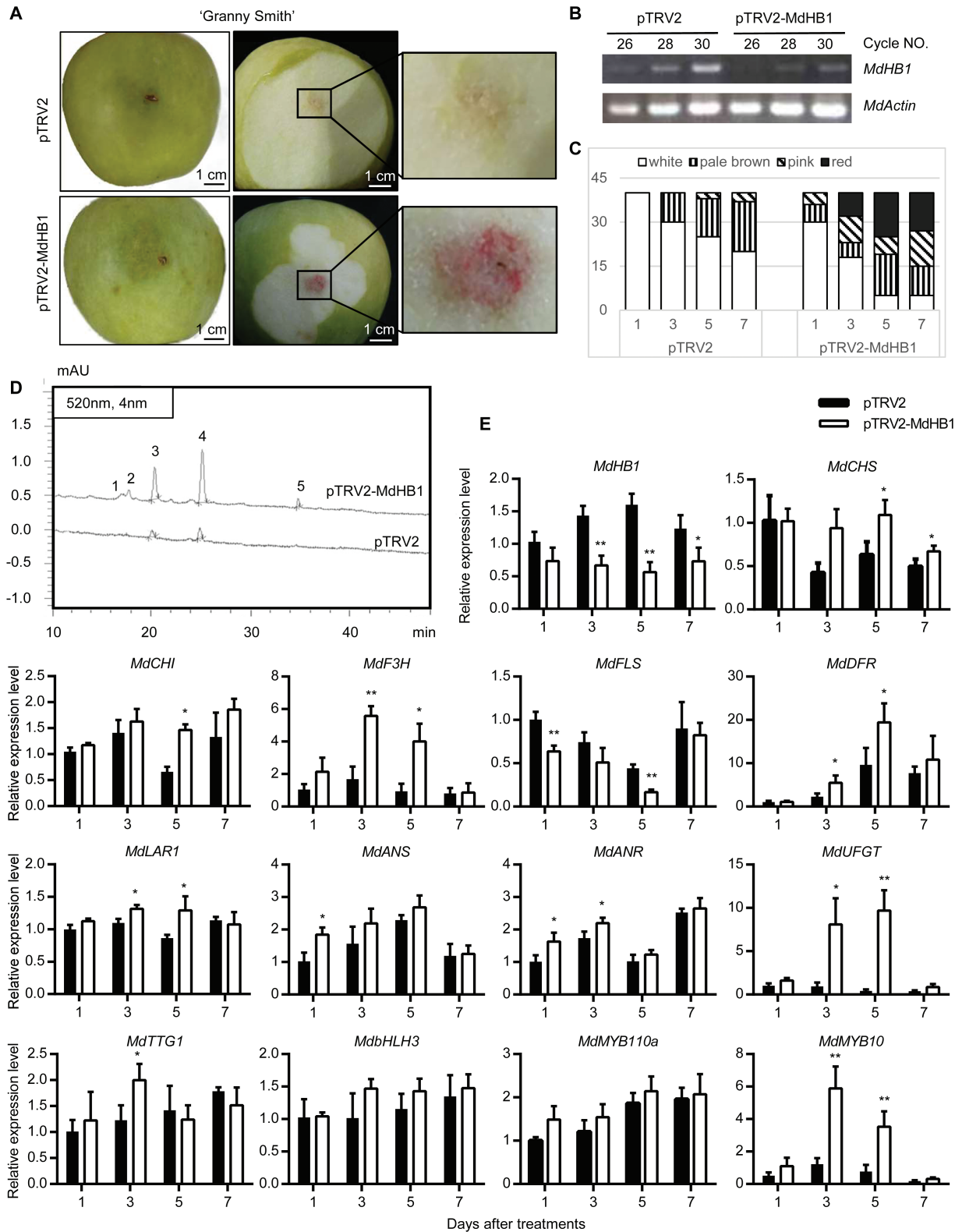


Fig. 4. *MdHB1* silencing causes a red coloration in 'Granny Smith' flesh. (A) Phenotypes of 'Granny Smith' after silencing *MdHB1* (pTRV2-MdHB1) for 5 d. Fruit inoculated with *Agrobacterium tumefaciens* containing empty vectors (pTRV2) were taken as a control. Injection areas are marked and magnified. (B) Semi-quantitative RT-PCR results of *MdHB1* transcripts in flesh tissues inside the injection areas. *MdActin* was used as a loading control. Cycle NO., cycle numbers. (C) Statistical results of the colored injection areas. The total number of injection regions at each time point was 40. (D) Flesh anthocyanin profiles of pTRV2-MdHB1 (top line) and pTRV2 (bottom line). Peaks identified from HPLC traces at 520 nm are as follows: 1, cyanidin 3-galactoside; 2, cyanidin 3-glucoside; 3, cyanidin 3-xyloside; 4, cyanidin 3-arabinoside; 5, unknown. Flesh tissues in (B) and (D) were collected 5 d after infiltration. (E) Expression analysis of *MdHB1*, flavonoid biosynthetic genes, and anthocyanin regulatory genes at four time points after VIGS treatments. Values are means \pm SD, $n=4$. Data were analyzed with Student's *t*-test (* $P<0.05$; ** $P<0.01$). (This figure is available in colour at JXB online.)

the level of *MdHb1* transcripts was clearly reduced relative to pTRV2 (Fig. 4B). The statistical results indicated that the colored areas in pTRV2-MdHb1 increased as the days passed, and their pigmentation intensity was increased on days 5 and 7 (Fig. 4C). The occasionally observed pink color in pTRV2-treated fruit may have been due to the wound caused by needle injection (Morker and Roberts, 2011; Li *et al.*, 2012).

To examine whether the red color was caused by anthocyanin accumulation (Espley *et al.*, 2007), HPLC analyses were performed with flesh tissues on day 5. These revealed two principal peaks, cyanidin 3-xyloside and cyanidin 3-arabinoside (Fig. 4D). Their contents in pTRV2-MdHb1-treated samples were 7.0- and 6.4-fold higher than those in pTRV2-treated samples, respectively (Table 1). The phenolic profile at 280 nm indicated that the contents of procyanidin B1 and epicatechin in pTRV2-MdHb1 were also higher than those in pTRV2 (Table 1). However, no clear flavonol signal was identified. Since proanthocyanidins and flavonols are colorless, we here focus on the accumulation of anthocyanins, which are mainly responsible for the red color in flesh.

Because anthocyanin content is regulated by both anthocyanin biosynthetic genes and MYB, bHLH, and WD40 TFs (see the Introduction), the transcription levels of those genes were determined at four time points after VIGS treatments. Relative to pTRV2, *MdHb1* transcription levels were decreased by pTRV2-MdHb1, particularly on days 3 and 5 (Fig. 4E). In contrast, excluding the flavonol gene (flavonol synthase, *FLS*), the mRNA levels of most biosynthetic genes, especially *F3H*, *DFR*, and *UFGT*, were elevated in pTRV2-MdHb1-treated fruit. At the same time, the expression of *MdMYB10* was clearly improved by *MdHb1* silencing, but this was not the case for *MdbHLH3*, *MdMYB10a*, and *MdTTG1*. Overall, the opposite expression trends of *MdHb1* and anthocyanin-related genes indicate that *MdHb1* is a negative regulator of anthocyanin. Since MBW complexes mainly regulate the late biosynthetic genes (Xu *et al.*, 2014), *MdDFR*, *MdUFGT*, and the key TF *MdMYB10* were selected for subsequent assays.

Overexpression of *MdHb1* disturbs the coloration in ‘Ballerina’ apple and ‘NC89’ tobacco in a tissue-specific manner

To know more about the regulatory role of *MdHb1* in apple, we selected ‘Ballerina’, whose flesh is red throughout fruit development, to transiently overexpress *MdHb1*. The color of flesh inside and outside of the injection areas was compared visually

Table 1. HPLC analyses of flavonoid contents in flesh in ‘Granny Smith’ after VIGS treatments for 5 ds

Phenolic (mg kg ⁻¹)		pTRV2	pTRV2-MdHb1
Anthocyanin	Cyanidin 3-xyloside	0.6 ± 0.08	4.8 ± 0.9
	Cyanidin 3-arabinoside	2.4 ± 0.5	17.8 ± 1.4
	Cyanidin 3-galactoside	ND	0.23 ± 0.09
	Cyanidin 3-glucoside	ND	0.43 ± 0.04
Proanthocyanidin	Procyanidin B1	543.30 ± 55.60	2246.67 ± 233.31
	Epicatechin	10.57 ± 1.72	58.13 ± 4.81

Values are means ±SD of three replicates. ND, not detected.

in the same fruit (Fig. 5A). About 10.6% (8 out of 75) of injection areas in the control (EmptyB; injected with empty vectors) showed a light red color, probably because the flesh color in fruit is inherently uneven. The high probability (57%, 43 out of 75) of a red color at the injection sites in *MdHb1*-overexpressing ‘Ballerina’ (OEB) suggested that *MdHb1* disturbed the accumulation of anthocyanin in ‘Ballerina’. The faded areas in OEB and the typical areas in EmptyB were collected to extract the total anthocyanin. Spectrophotometric quantification demonstrated that the anthocyanin content in OEB was lower than that in EmptyB, albeit not significantly (Fig. 5B). Because *MdHb1* silencing greatly increased the expression of *MdDFR*, *MdUFGT*, and *MdMYB10* (Fig. 4E), transcripts of these four genes inside the typical injection areas were examined by quantitative RT-PCR. The results showed that OEB significantly up-regulated the expression of *MdHb1*, but slightly down-regulated the mRNA levels of *MdDFR*, *MdUFGT*, and *MdMYB10* relative to EmptyB (Fig. 5C).

To identify further the function of *MdHb1* in planta, 35S:*MdHb1* was stably introduced into ‘NC89’, whose flowers are red, to generate transgenic tobacco lines overexpressing *MdHb1* (OETs). Thirty independent OETs were obtained. After characterization of the expression of *MdHb1* in all T₀ lines, eight lines were selected to generate T₁ lines. The color of the corolla of open flowers in five T₁ lines was faded (Fig. 5D). No color variation was found in sepals, leaves, and stems. Spectrophotometric quantification with the corolla of flowers in full bloom demonstrated that OETs contained a lower anthocyanin content than wild-type plants (WTTs) (Fig. 5E). Semi-quantitative RT-PCR tests revealed that *MdHb1* mRNA was abundant in OET-1, but undetectable in WTT-1 (Fig. 5F). Further quantitative RT-PCR showed that transcripts of *DFR*, *UFGT*, and *MYB10* in tobacco flowers were all markedly down-regulated by the overexpression of *MdHb1* relative to WTT-1 (Fig. 5G).

MdHb1 and *MdMYB10* inversely regulate the promoter activities of *MdUFGT* and *MdDFR*

Having determined that there is a close connection among *MdHb1*, *MdMYB10*, *MdDFR*, and *MdUFGT*, we investigated whether these two TFs control the expression of these two synthetic genes. First, we performed transient dual-luciferase detections. The injection of ProUFGT-LUC/ProDFR-LUC produced some LUC activities due to endogenous TFs in tobacco (Ban *et al.*, 2007; Pattanaik *et al.*, 2010; Zhou *et al.*, 2015). These activities were significantly enhanced by *MdMYB10* (up-regulated by 2.3- and 1.8-fold, respectively). Further addition of *MdbHLH3* and *MdTTG1* strengthened these activities by 7.4-fold (1.8-fold) relative to ProUFGT-LUC (ProDFR-LUC) alone (Fig. 6A, B). In contrast, the participation of *MdHb1* always weakened such activation, especially for ProUFGT. These characters were also detected from bioluminescent images of firefly LUC activities (Fig. 6C, D).

At the same time, ProUFGT/ProDFR-GUS analyses demonstrated that the expression of GUS was up-regulated by *MdMYB10*, but down-regulated by *MdHb1* (Fig. 6E, F). The inhibitory effect of *MdHb1* on ProUFGT was stronger than that on ProDFR.

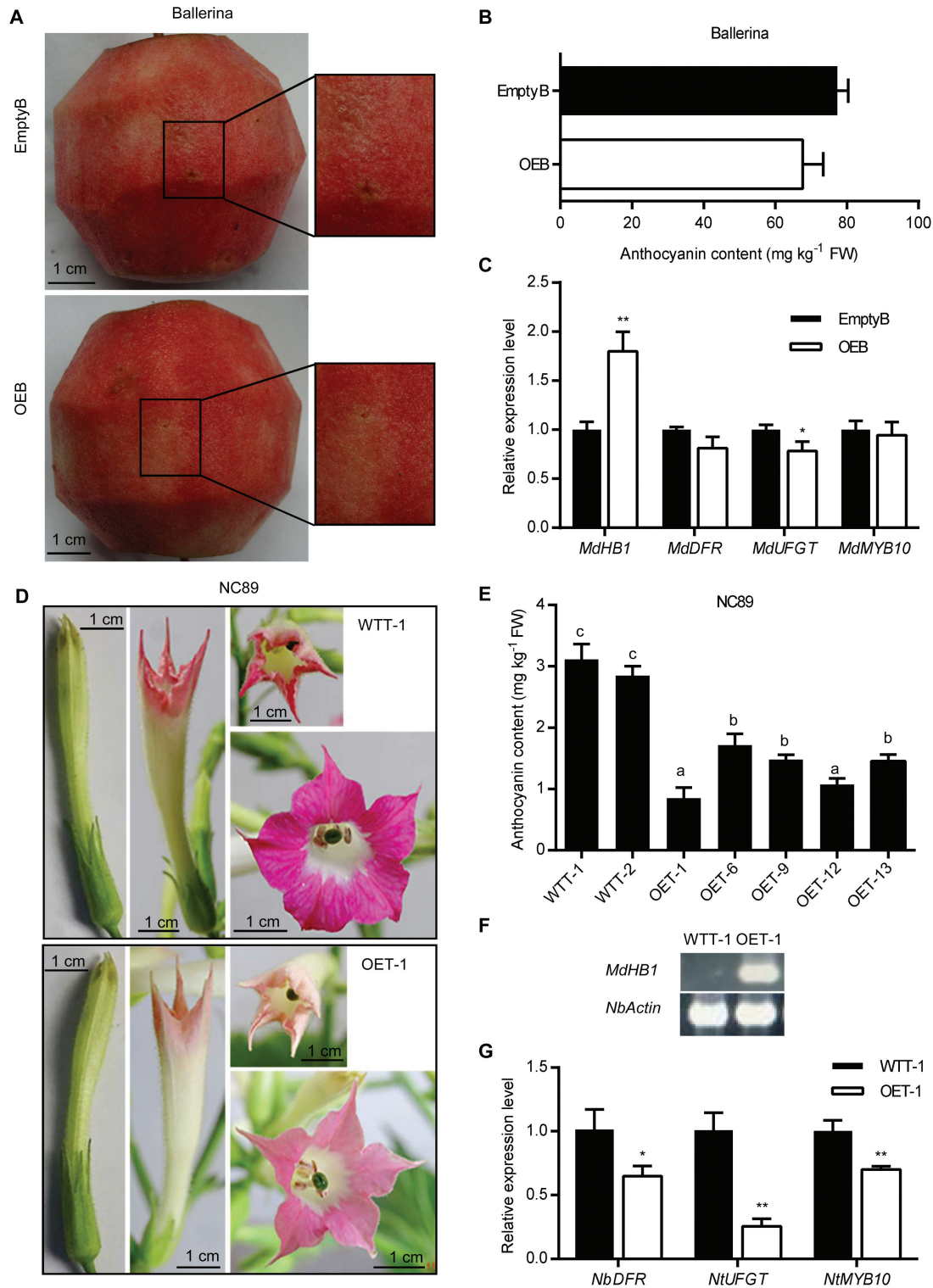


Fig. 5. Overexpression of *MdHB1* disturbs the coloration in ‘Ballerina’ and ‘NC89’ in a tissue-specific manner. (A) The flesh phenotypes of *MdHB1*-overexpressing ‘Ballerina’ (OEB) and the control (EmptyB) 5 d after infiltration. Typical injection areas are marked and magnified. (B and C) Anthocyanin contents and the expression of related genes in the flesh of EmptyB and OEB on day 5. (D) Phenotypes of ‘NC89’ flowers in wild-type line 1 (WTT-1) and *MdHB1*-overexpressing line 1 (OET-1). (E) Anthocyanin levels in the corolla of open flowers in different tobacco lines. (F) Semi-quantitative RT–PCR results of *MdHB1* expression in the flowers of WTT-1 and OET-1. *NbActin* was used as a loading control. (G) Quantitative RT–PCR results of the expression of *DFR*, *UGFT*, and *MYB10*. Values are means \pm SD, $n=3$. Data in (B), (C) and (G) were analyzed with Student’s *t*-test. * $P<0.05$; ** $P<0.01$. Data in (E) were analyzed with one-way ANOVA. Different letters denote statistical significance at $P<0.05$. (This figure is available in colour at JXB online.)

To investigate whether *MdHB1* regulated *DFR*/*UGFT* directly, Y1H tests were designed. Because no identical binding motif for HD-Zip was found in Pro*DFR* and Pro*UGFT* (Sessa *et al.*, 1993; Lin *et al.*, 2008), the Y1H tests were

performed with the whole promoter sequences. The results showed that *MdMYB10* bound to Pro*DFR*, but no combination was detected between *MdHB1* and Pro*UGFT*/Pro*DFR* (Supplementary Fig. S4).

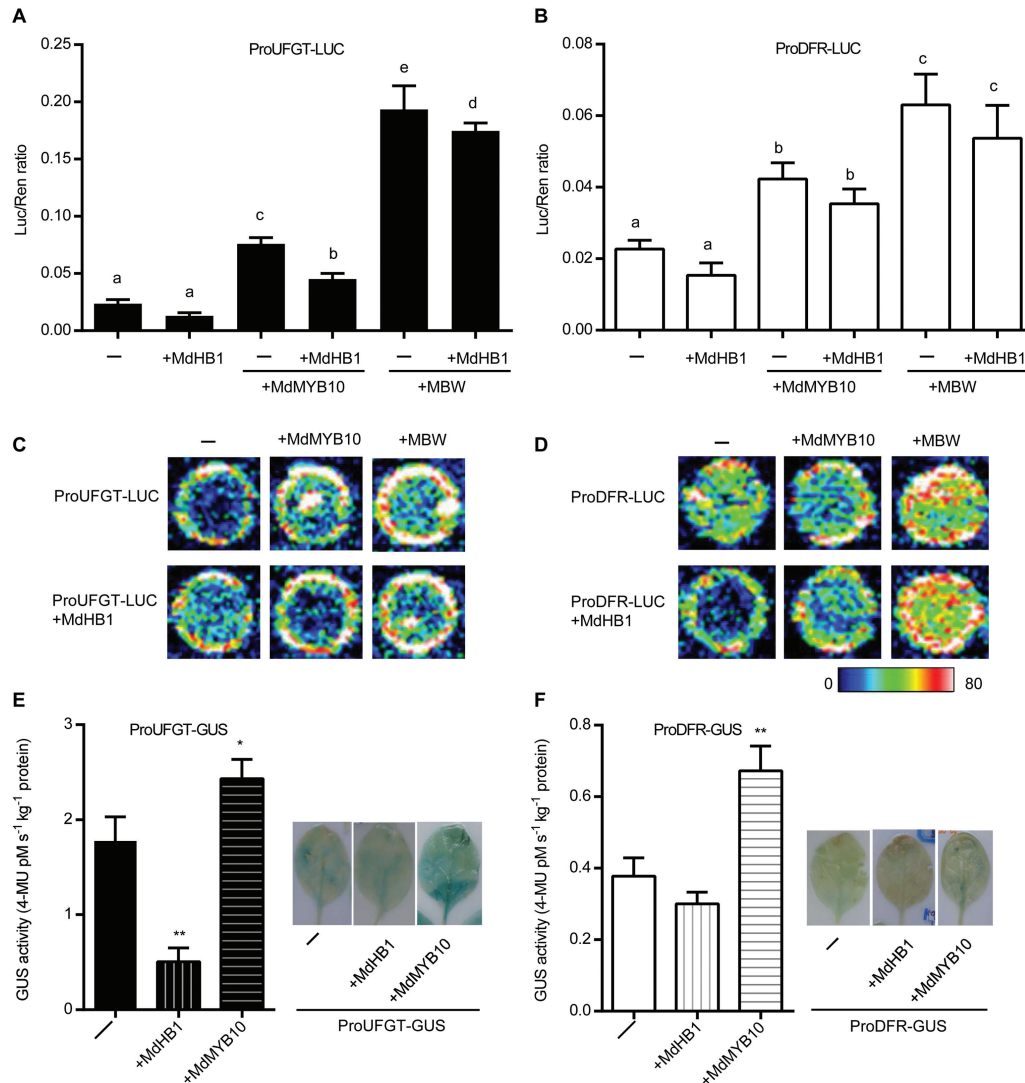


Fig. 6. Activation and repression assays of *MdDFR* and *MdUFGT* promoters (ProDFR and ProUFGT). (A and B) Transient dual-luciferase detections of ProDFR and ProUFGT in *N. benthamiana* leaves. MBW, MYB10, bHLH, and WD40 transcription factors. (C and D) Typical CCD image of luciferase (LUC) reporters in (A) and (B), respectively. The pseudocolor bar below shows the range of luminescence intensity in each image. Experiments were repeated four times. (E and F) Fluorescent analysis and typical histochemical stain of β -glucuronidase (GUS) activity in 'NC89' leaves. 4-MU, 4-methylumbelliferone. Six leaves were stained. Values are means \pm SD, $n=4$. Different letters in (A) and (B) denote statistical significance (one-way ANOVA, $P<0.05$). Data in (E) and (F) were analyzed with Student's *t*-test (* $P<0.05$; ** $P<0.01$).

Simultaneous silencing of *MdHB1* and *MdMYB10* blocks the coloration in flesh

Because the expression of *MdMYB10* was markedly altered in *MdHB1*-silenced tissues (Fig. 4E) and *MdMYB10* contributes to the red color in flesh (Espley *et al.*, 2007), *MdMYB10* might be an important factor for the coloration. To confirm this, a VIGS strategy was adopted to silence *MdMYB10* (Fig. 7A). The decline in mRNA level revealed that pTRV2-*MdMYB10* could effectively decrease the level of *MdMYB10* transcripts (Fig. 7B). Simultaneous silencing of *MdHB1* and *MdMYB10* hindered the red coloration caused by pTRV2-*MdHB1* treatment, and also reduced the expression of both *MdHB1* and *MdMYB10*. At the same time, the levels of *MdDFR* and *MdUFGT* transcripts were significantly reduced relative to that of pTRV2.

Considering the interfering effect of *MdHB1* on promoter-reporter assays (Fig. 6), there may be a regulatory network

between *MdHB1* and *MdMYB10*. Thus, ProMYB and ProHB were cloned to drive the reporter gene GUS. GUS activity assays and histochemical stains revealed that both ProMYB and ProHB had promoter activities and these activities were significantly suppressed by both *MdHB1* and *MdMYB10* (Fig. 7C, D). The strong activity of ProMYB-GUS may result from the specific 5'-untranslated region (UTR) pyrimidine-rich stretch (Supplementary Fig. S1), which can increase transcriptional activity (Daraselia *et al.*, 1996).

MdHB1 interacts with MBW TFs

Since *MdHB1* did not bind to ProUFGT/ProDFR, its regulation of anthocyanin biosynthesis may be mediated by other proteins (e.g. MYB, bHLH, and WD40 TFs). To clarify this, Y2H tests were performed. A previous study reported that *MdHB1* could be autoactivated in yeast, while the C-terminal region truncated *MdHB1* protein *MdHB1* Δ has

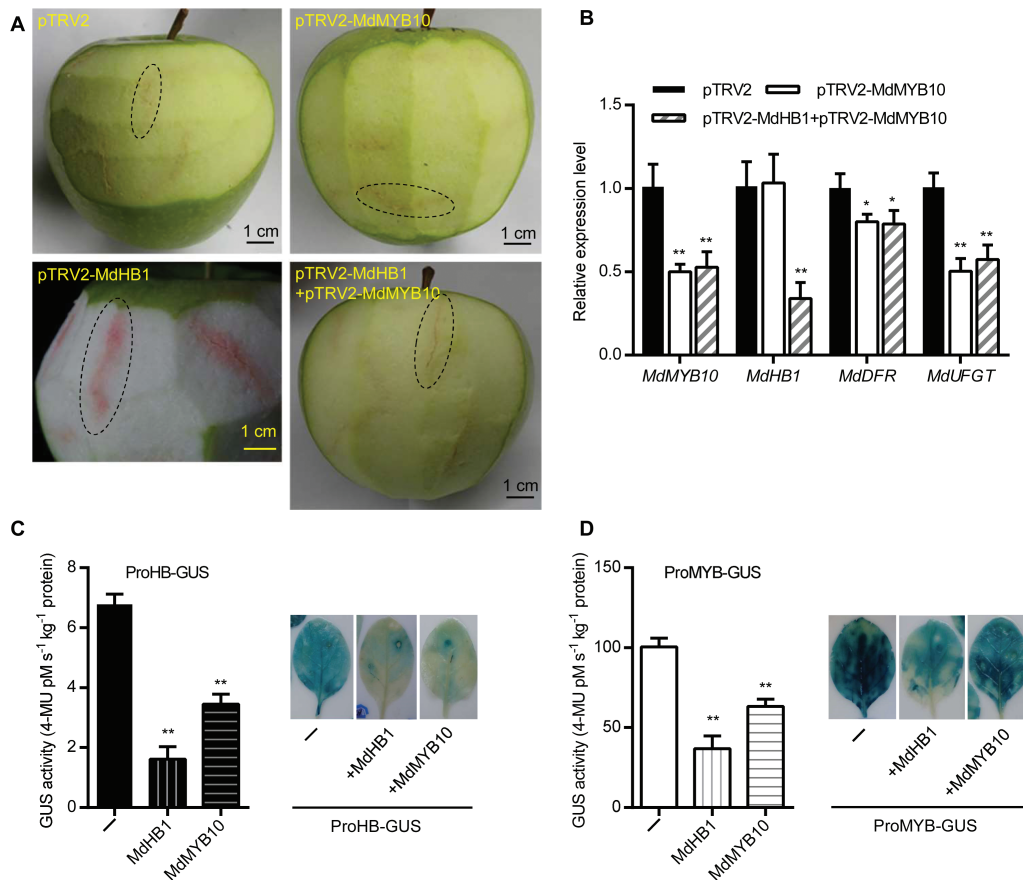


Fig. 7. Regulation of flesh coloration is fine-tuned by MdMYB10 and MdHb1 in 'Granny Smith'. (A) Phenotypes of 'Granny Smith' after VIGS treatments for 5 d. (B) Expression levels of *MdMYB10*, *MdHb1*, *MdDFR*, and *MdUGT* in typical injection areas (marked with dashed lines). (C and D) Fluorescent analysis of promoter activity and typical histochemical stain in 'NC89' leaves. Six leaves were stained. Values are means \pm SD, $n=4$. Data were analyzed with Student's *t*-test. * $P<0.05$; ** $P<0.01$. (This figure is available in colour at JXB online.)

no activating capacity (Liu *et al.*, 2015). Here, Y2H assays with BD-MdHb1 Δ showed that MdHb1 interacted with MdHb1, MdMYB10, MdbHLH3, and MdTTG1 (Fig. 8A).

Because the C-terminus is important for the binding activities of HD-Zip members (Arce *et al.*, 2011; Capella *et al.*, 2014), the full-length *MdHb1* was used to perform BiFC assays to reconfirm those interactions (Li *et al.*, 2012; Yu *et al.*, 2013; Chen *et al.*, 2016). Physical interactions were clearly observed between MdHb1 and three TFs, namely MdHb1, MdMYB10, and MdTTG1; the interaction between MdHb1 and MBW TFs was particularly strong (Fig. 8B). However, the YFP signal showing the interaction between MdHb1 and MdbHLH3 was too weak to be detected in the whole cell, which was consistent with the Y2H results. Notably, with MdHb1, YFP fluorescence was localized in the cytoplasm, except for with the empty pSPYNE vector (NE), which was a negative control and failed to give any YFP signal.

Discussion

HD-Zip I protein MdHb1 negatively regulates anthocyanin biosynthesis

The HD-Zip I protein MdHb1, isolated from 'Granny Smith', shares the greatest sequence similarity with LeHb1 in tomato

(Fig. 2), which is involved in the regulation of fruit development and ripening (Lin *et al.*, 2008). The silencing of *MdHb1* causes a delay in ethylene production in mature apple fruit (Wen *et al.*, 2015), indicating that MdHb1 is functionally homologous to LeHb1. Taking this together with the feature that *MdHb1* is constitutively expressed in 'Granny Smith' (Fig. 3), we assume that MdHb1 possesses multiple functions in plant growth and fruit ripening, as previously reported for other HD-Zip I members (Hur *et al.*, 2015; Chen *et al.*, 2016; Hu *et al.*, 2016; Kovalchuk *et al.*, 2016).

VIGS is considered to be a powerful tool for investigating gene function *in vivo* (Sun *et al.*, 2016), and has been successfully used in fruit of pear (Z. Wang *et al.*, 2013; Zhai *et al.*, 2016), tomato (Lin *et al.*, 2008), strawberry (*Fragaria×ananassa*) (Jia *et al.*, 2013; Medina-Puche *et al.*, 2014), and apple (Li *et al.*, 2012; Li *et al.*, 2016). Based on our previous work, we noticed that the silencing of *MdHb1* using VIGS led to a red coloration in mature 'Granny Smith' (Fig. 4A). Early studies also showed that *RhHb1* (HD-Zip I) impacted the flower color of rose (*Rosa hybrida*) (Lu *et al.*, 2014); in addition, VviATHB6/13 (HD-Zip I) bound to the promoter of the flavonoid 3'-hydroxylase-encoding gene to regulate the flavonoid pathway in grape (*Vitis vinifera*) (Sun *et al.*, 2015). Taking these findings together, we speculate that HD-Zip I TF MdHb1 possesses a novel feature of an involvement in apple flesh coloration.

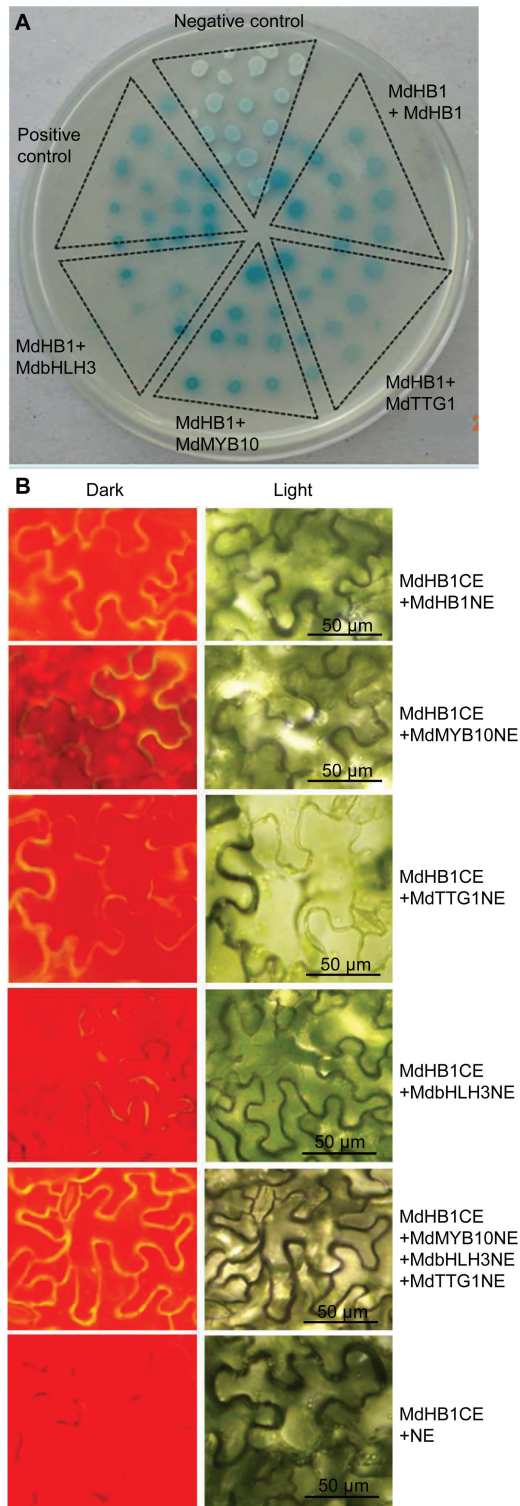


Fig. 8. Protein–protein interactions between MdHB1 and MBW transcription factors. (A) Physical interactions in the yeast two-hybrid system. Positive control, pGADT7-T+pGBKT7-53. Negative control, pGADT7-T+pGBKT7-Lam. (B) Bimolecular fluorescence complementation assay in *N. benthamiana* leaves. Except for with MBW components (3:1:1:1), MdHB1CE were mixed with other NE series at a volume ratio of 1:1. Experiments were repeated four times. (This figure is available in colour at JXB online.)

HPLC analyses with VGIS-treated samples revealed that the coloration in flesh results from the accumulation of anthocyanin. Anthocyanin content increased or decreased after the

down- or up-regulation of *MdHB1* transcripts (Figs 4D, 5B). Consistent with this, *MdHB1* and anthocyanin biosynthetic genes, especially *MdDFR* and *MdUFGT*, displayed the opposite transcriptional profiles (Fig. 4E). Therefore, we suggest that MdHB1 is a negative regulator of anthocyanin, just as in the cases of PhMYBx (Albert *et al.*, 2011) and FaMYB1 (Aharoni *et al.*, 2001). The restricted impact on red-fleshed ‘Ballerina’ (Fig. 5B) indicates that the function of MdHB1 is limited and MdHB1 has little effect on anthocyanin degradation, which has rarely been studied (Fang *et al.*, 2015). Furthermore, its suppressive function observed in ‘NC89’ (Fig. 5D) indicates that the mechanism by which MdHB1 inhibits anthocyanin biosynthesis in tobacco and apple may be the same. However, the negative regulation of MdHB1 is restricted to the flesh of apple and the flower of tobacco, indicating that MdHB1 plays a tissue-specific role, similar to the case of SVP3 (Wu *et al.*, 2014).

Notably, the principal anthocyanin elevated in *MdHB1*-silenced tissues was cyanidin 3-arabinoxide (Fig. 4D), not cyanidin 3-galactoside. The latter is the main regulator of the red color in most apple cultivars under natural conditions (Lister *et al.*, 1997; Espley *et al.*, 2007; Chagne *et al.*, 2013; Zhang *et al.*, 2013; Wang *et al.*, 2015). A previous study documented that UFGT controls the terminal step of anthocyanin biosynthesis (Fig. 1), and specifically transfers glycosides from various sugar donors to the 3-position of flavonoids (Lister *et al.*, 1997). Together with the dramatically altered *MdUFGT* transcripts (Fig. 4E), we assume that *MdHB1* silencing alters the UFGT enzyme to exhibit high activity with arabinose, not with galactose, which subsequently leads to a change of cyanidin series. More evidence in support of this should be obtained in future studies.

HPLC analyses also showed that *MdHB1* affects the flesh content of proanthocyanidins (Table 1), the dominant phenolic compounds in apple fruit (Takos *et al.*, 2006b; Jakobek *et al.*, 2013). However, its connection with the expression of proanthocyanidin-related genes (e.g. *LAR1* and *ANR*) appeared to be weak (Fig. 4E; Table 1). One possible explanation is that other members in the *LAR* and *ANR* families may also regulate the content of proanthocyanidins (Takos *et al.*, 2006b). In addition, no detectable flavonol in flesh is in line with its low content in the flesh of many apple genotypes, because flavonols are usually found in peel (Łata *et al.*, 2009; Chen *et al.*, 2012; Jakobek *et al.*, 2013). Taking these findings together, MdHB1 negatively regulates the accumulation of proanthocyanin and anthocyanin. Its regulation of anthocyanin accumulation is mainly restricted to the suppression of anthocyanin biosynthesis by inhibiting the expression of *MdDFR/MdUFGT* in specific tissues.

MdMYB10 is necessary for flesh coloration

Besides *MdDFR/MdUFGT*, the levels of *MdMYB10* transcripts also changed markedly (Fig. 4E), implicating MdMYB10 in the red coloration (Espley *et al.*, 2007; Wang *et al.*, 2015). The simultaneous silencing of *MdMYB10* and *MdHB1* produced no pigmentation (Fig. 7A), suggesting that MdMYB10 is essential for red coloration, which involves activating the expression of *MdDFR/MdUFGT*

(Fig. 6) (Talos *et al.*, 2006a; Espley *et al.*, 2007). This type of regulation is well documented. First, PpMYB10 in peach activates the expression of both *PpDFR* and *PpUFGT* (Zhou *et al.*, 2015). Secondly, PcMYB10 in pear binds to the promoter of *PcUFGT* (Z. Wang *et al.*, 2013; Zhai *et al.*, 2016). In addition, MdMYB1 interacts with MdbHLH3, which binds specifically to the promoters of *MdDFR* and *MdUFGT* (Xie *et al.*, 2012). Lastly, MdMYB10, MdbHLH3, and MdTTG1 significantly enhance the promoter activities of *MdDFR* and *MdUFGT* (Fig. 6) (Espley *et al.*, 2007). Taking these findings together, the key TF MdMYB10 combines with other TFs, such as MdbHLH3 and MdTTG1, to activate the expression of *MdDFR* and *MdUFGT*, leading to the accumulation of anthocyanin.

Possible mechanism behind the negative regulation of anthocyanin biosynthesis by MdHB1

Notably, MdHB1 did not bind to the promoter of *MdDFR*/*MdUFGT* (Fig. S4), indicating that the negative regulation of the anthocyanin biosynthetic genes *MdDFR* and *MdUFGT* by MdHB1 is indirect. Therefore, MdHB1 may regulate anthocyanin biosynthesis via its partners.

First, consistent with the hetero- or homodimers formed by other HD-Zip proteins (Sessa *et al.*, 1993; Wang *et al.*, 2005; Rice *et al.*, 2014), MdHB1 interacts with another copy of itself (Fig. 8) to form a homodimer, which could promote its transcriptional specificity (Papadopoulos *et al.*, 2012). The formation of a homodimer in the cytoplasm (Fig. 8B) is consistent with the distribution of GFP fluorescence controlled by both 35S and ProHB (Fig. 3A). These subcellular localization results differ from those for some HD-Zip TFs found in the nucleus (Wang *et al.*, 2005; Zhao *et al.*, 2014; Gao *et al.*, 2016), but are similar to those of other HD-Zip members, such as OsHOX9 (Ai *et al.*, 2014), GbML1 (Zhang *et al.*, 2010), and AtGL2 (Zhao *et al.*, 2008), which possess cytoplasm localization signals under the control of 35S. Since HD-Zip domain and N-terminal amino acids are associated with cellular localization (Rice *et al.*, 2014; Gao *et al.*, 2016), our observations with the full-length *MdHB1* indicate that MdHB1 plays a role in both the cytoplasm and the nucleus.

Secondly, MdHB1 interacts with MBW TFs in the cytoplasm (Fig. 8B). This is consistent with the BiFC results obtained in recent studies. First, Mict (HD-Zip I) interacts with CsTTG1 (WD40 protein) only in the cytoplasm (Chen *et al.*, 2016). Secondly, StERF3, a TF located only in the nucleus under the control of 35S, interacts with some proteins in the cytoplasm (Tian *et al.*, 2015). Previous BiFC tests showed that MdMYB1 interacts with MdbHLH3 in the nucleus (Xie *et al.*, 2012), where the interaction of MdbHLH3 and MdTTG1 is also observed (An *et al.*, 2012). Therefore, we propose that MdHB1 alters the subcellular localization of the co-expressed MBW TFs.

Relocation of proteins is a common activity in plants (Tian *et al.*, 2015). It can be caused by their co-expressed proteins (Zhang *et al.*, 2010). One example, the cytoplasmic protein DIP1, is transferred to the nucleus after its co-transformation

with DBF1 (Saleh *et al.*, 2006). Secondly, light alters the subcellular location of phytochrome photoreceptors (Klose *et al.*, 2015). Thus, the light response elements (Box 4, Sp1, and G-box; Supplementary Fig. S1) in ProMYB10 indicated that the location of MdMYB10 and MdHB1 might be affected by light. Moreover, post-translational modifications such as phosphorylation can activate proteins and translocate them from the cytoplasm to the nucleus (P. Wang *et al.*, 2013; Tian *et al.*, 2015). Both MdHB1 (Li, 2014) and MdbHLH3 (Li *et al.*, 2012) are reported to be involved in phosphorylation. Taking these findings together, it is likely that MdHB1 performs its suppressive function via the recruitment of MdMYB10, MdbHLH3, and MdTTG1 to the cytoplasm. However, further experiments are required to reveal whether this relocation involves phosphorylation or some other mechanisms.

In addition to the protein–protein interaction described above, MdHB1 and MdMYB10 negatively regulate each other (Fig. 7C, D). The negative regulation of *MdMYB10* itself in white-fleshed apple differs from its activation in red-fleshed apple (Espley *et al.*, 2009). The form of regulation varies markedly among HD-Zip members (Ré *et al.*, 2014; Rice *et al.*, 2014), similarly to the case between MBW and HD-Zip TFs (Morohashi *et al.*, 2007; Zhao *et al.*, 2008; Khosla *et al.*, 2014). All of these features provide clues to how white flesh is generated in ‘Granny Smith’.

In summary, we have established a working model to show the association of MdHB1 with anthocyanin biosynthesis in white-fleshed ‘Granny Smith’ (Fig. 9). In mature fruit under normal conditions, MdHB1 recruits MBW TFs to the cytoplasm. These combinations indirectly suppress the transcription of *MdDFR* and *MdUFGT*, encoding key enzymes in anthocyanin biosynthesis. When *MdHB1* mRNA levels are decreased by RNAi approaches (e.g. VIGS), the MBW TFs are released to activate the expression of *MdDFR* and *MdUFGT*, leading to red pigmentation in the flesh.

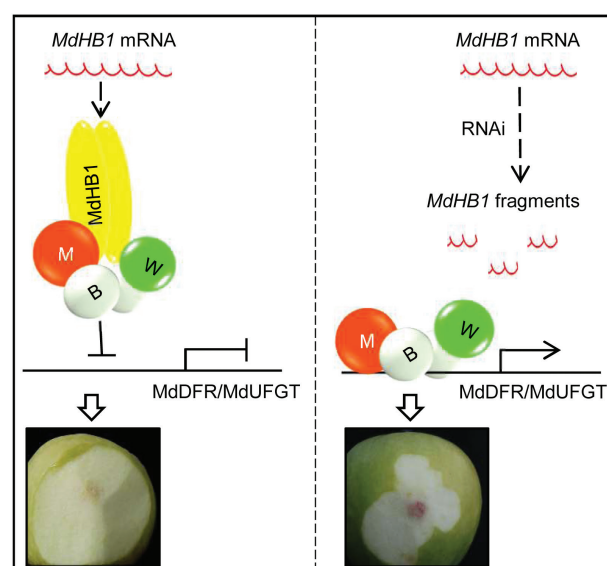


Fig. 9. A model for the negative regulation of anthocyanin biosynthesis by MdHB1 in ‘Granny Smith’. M, MdMYB10; B, MdbHLH3; W, MdTTG1. (This figure is available in colour at JXB online.)

Supplementary data

Supplementary data are available at *JXB* online.

Data S1. GenBank accession numbers for HD-Zip proteins in Fig. 1.

Table S1. Primers used in this study.

Fig. S1. Diagram of promoter structures and *cis*-regulatory elements within them.

Fig. S2. Sequence alignment of MdHB1 from 'Granny Smith' (GS) and 'Royal Gala' (RG).

Fig. S3. Diagram of the VIGS system and the silencing effects of *MdHB1*.

Fig. S4. Yeast one-hybrid results with the *MdDFR*/*MdUGT* promoter on SD-Leu/AbA plates.

Acknowledgements

We thank Professor Mingyu Han, Zhengyang Zhao, and Bingzhi Li for providing the apples, Pengmin Li for assistance in HPLC analysis, Yan Xu and Wangjin Lu (South China Agricultural University) for the gifts of BiFC and dual-luciferase assay vectors, respectively, and Dr Rui Zhai, Libo Xing, Yanrong Lyv, and Kaili Chen for their advice on manuscript correction. We express our deepest gratitude to Dr Xilong Chen for his support in many ways. This work was supported by the Modern Agricultural Industry Technology System of China for apple (Z225020701), the National Science Foundation of China (31501724), and the China Postdoctoral Science Foundation (2015M580881).

References

- Aharoni A, De Vos CH, Wein M, Sun Z, Greco R, Kroon A, Mol JN, O'Connell AP. 2001. The strawberry FaMYB1 transcription factor suppresses anthocyanin and flavonol accumulation in transgenic tobacco. *The Plant Journal* **28**, 319–332.
- Ahmed SS, Gong ZH, Ji JJ, Yin YX, Xiao HJ, Khan MA, Rehman A, Ahmad I. 2012. Construction of the intermediate vector pVBG2307 by incorporating vital elements of expression vectors pBI121 and pBI221. *Genetics and Molecular Research* **11**, 3091–3104.
- Ai L, Shen A, Gao Z, Li Z, Sun Q, Li Y, Luan W. 2014. Reverse genetic analysis of transcription factor OsHox9, a member of homeobox family, in rice. *Rice Science* **21**, 312–317.
- Albert NW, Davies KM, Lewis DH, et al. 2014. A conserved network of transcriptional activators and repressors regulates anthocyanin pigmentation in eudicots. *The Plant Cell* **26**, 962–980.
- Albert NW, Lewis DH, Zhang H, Schwinn KE, Jameson PE, Davies KM. 2011. Members of an R2R3-MYB transcription factor family in *Petunia* are developmentally and environmentally regulated to control complex floral and vegetative pigmentation patterning. *The Plant Journal* **65**, 771–784.
- Alipour B, Rashidkhani B, Edalati S. 2016. Dietary flavonoid intake, total antioxidant capacity and lipid oxidative damage: a cross-sectional study of Iranian women. *Nutrition* **32**, 566–572.
- An XH, Tian Y, Chen KQ, Wang XF, Hao YJ. 2012. The apple WD40 protein MdTTG1 interacts with bHLH but not MYB proteins to regulate anthocyanin accumulation. *Journal of Plant Physiology* **169**, 710–717.
- Arce AL, Raineri J, Capella M, Cabello JV, Chan RL. 2011. Uncharacterized conserved motifs outside the HD-Zip domain in HD-Zip subfamily I transcription factors; a potential source of functional diversity. *BMC Plant Biology* **11**, 42.
- Balázs A, Tóth M, Blazics B, Héthelyi É, Szarka S, Ficsor E, Ficzek G, Lemberkovics É, Blázovics A. 2012. Investigation of dietary important components in selected red fleshed apples by GC-MS and LC-MS. *Fitoterapia* **83**, 1356–1363.
- Ban Y, Honda C, Hatsuyama Y, Igarashi M, Bessho H, Moriguchi T. 2007. Isolation and functional analysis of a MYB transcription factor gene that is a key regulator for the development of red coloration in apple skin. *Plant and Cell Physiology* **48**, 958–970.
- Baudry A, Caboche M, Lepiniec L. 2006. TT8 controls its own expression in a feedback regulation involving TTG1 and homologous MYB and bHLH factors, allowing a strong and cell-specific accumulation of flavonoids in *Arabidopsis thaliana*. *The Plant Journal* **46**, 768–779.
- Bondonno CP, Yang X, Croft KD, et al. 2012. Flavonoid-rich apples and nitrate-rich spinach augment nitric oxide status and improve endothelial function in healthy men and women: a randomized controlled trial. *Free Radical Biology and Medicine* **52**, 95–102.
- Boss PK, Davies C, Robinson SP. 1996. Analysis of the expression of anthocyanin pathway genes in developing *Vitis vinifera* L. cv Shiraz grape berries and the implications for pathway regulation. *Plant Physiology* **111**, 1059–1066.
- Capella M, Ré DA, Arce AL, Chan RL. 2014. Plant homeodomain-leucine zipper I transcription factors exhibit different functional AHA motifs that selectively interact with TBP or/and TFIIB. *Plant Cell Reports* **33**, 955–967.
- Chagné D, Lin-Wang K, Espley RV, et al. 2013. An ancient duplication of apple MYB transcription factors is responsible for novel red fruit-flesh phenotypes. *Plant Physiology* **161**, 225–239.
- Chen C, Yin S, Liu X, et al. 2016. The WD-repeat protein CsTTG1 regulates fruit wall formation through interaction with the homeodomain-leucine zipper I protein Mict. *Plant Physiology* **171**, 1156–1168.
- Chen C, Zhang D, Wang Y, Li P, Ma F. 2012. Effects of fruit bagging on the contents of phenolic compounds in the peel and flesh of 'Golden Delicious', 'Red Delicious', and 'Royal Gala' apples. *Scientia Horticulturae* **142**, 68–73.
- Daraseelia ND, Tarchevskaya S, Narita JO. 1996. The promoter for tomato 3-hydroxy-3-methylglutaryl coenzyme A reductase gene 2 has unusual regulatory elements that direct high-level expression. *Plant Physiology* **112**, 727–733.
- Espley RV, Brendolise C, Chagné D, et al. 2009. Multiple repeats of a promoter segment causes transcription factor autoregulation in red apples. *The Plant Cell* **21**, 168–183.
- Espley RV, Hellens RP, Putterill J, Stevenson DE, Kuttly-Amma S, Allan AC. 2007. Red colouration in apple fruit is due to the activity of the MYB transcription factor, MdMYB10. *The Plant Journal* **49**, 414–427.
- Fang F, Zhang XL, Luo HH, et al. 2015. An intracellular laccase is responsible for epicatechin-mediated anthocyanin degradation in litchi fruit pericarp. *Plant Physiology* **169**, 2391–2408.
- Faramarzi S, Pacifico S, Yadollahi A, Lettieri A, Nocera P, Piccolella S. 2015. Red-fleshed apples: old autochthonous fruits as a novel source of anthocyanin antioxidants. *Plant Foods for Human Nutrition* **70**, 324–330.
- Faramarzi S, Yadollahi A, Soltani BM. 2014. Preliminary evaluation of genetic diversity among Iranian red fleshed apples using microsatellite markers. *Journal of Agricultural Science and Technology* **16**, 373–384.
- Gao S, Fang J, Xu F, Wang W, Chu C. 2016. Rice HOX12 regulates panicle exertion by directly modulating the expression of ELONGATED UPPERMOST INTERNODE1. *The Plant Cell* **28**, 680–695.
- Gonzalez A, Zhao M, Leavitt JM, Lloyd AM. 2008. Regulation of the anthocyanin biosynthetic pathway by the TTG1/bHLH/MYB transcriptional complex in *Arabidopsis* seedlings. *The Plant Journal* **53**, 814–827.
- Hellens RP, Allan AC, Friel EN, Bolitho K, Grafton K, Templeton MD, Karunairatnam S, Gleave AP, Laing WA. 2005. Transient expression vectors for functional genomics, quantification of promoter activity and RNA silencing in plants. *Plant Methods* **1**, 13.
- Hu CG, Honda C, Kita M, Zhang Z, Tsuda T, Moriguchi T. 2002. A simple protocol for RNA isolation from fruit trees containing high levels of polysaccharides and polyphenol compounds. *Plant Molecular Biology Reporter* **20**, 69–69.
- Hu T, Ye J, Tao P, Li H, Zhang J, Zhang Y, Ye Z. 2016. The tomato HD-Zip I transcription factor SlHZ24 modulates ascorbate accumulation through positive regulation of the D-mannose/L-galactose pathway. *The Plant Journal* **85**, 16–29.
- Hur YS, Um JH, Kim S, et al. 2015. *Arabidopsis thaliana* homeobox 12 (ATHB12), a homeodomain-leucine zipper protein, regulates leaf growth by promoting cell expansion and endoreduplication. *New Phytologist* **205**, 316–328.
- Jaakola L. 2013. New insights into the regulation of anthocyanin biosynthesis in fruits. *Trends in Plant Science* **18**, 477–483.

- Jakobek L, García-Villalba R, Tomás-Barberán FA.** 2013. Polyphenolic characterisation of old local apple varieties from Southeastern European region. *Journal of Food Composition and Analysis* **31**, 199–211.
- Jia HF, Lu D, Sun JH, Li CL, Xing Y, Qin L, Shen YY.** 2013. Type 2C protein phosphatase ABI1 is a negative regulator of strawberry fruit ripening. *Journal of Experimental Botany* **64**, 1677–1687.
- Khosla A, Paper JM, Boehler AP, Bradley AM, Neumann TR, Schrick K.** 2014. HD-Zip proteins GL2 and HDG11 have redundant functions in Arabidopsis trichomes, and GL2 activates a positive feedback loop via MYB23. *The Plant Cell* **26**, 2184–2200.
- Klose C, Viczián A, Kircher S, Schäfer E, Nagy F.** 2015. Molecular mechanisms for mediating light-dependent nucleo/cytoplasmic partitioning of phytochrome photoreceptors. *New Phytologist* **206**, 965–971.
- Kovalchuk N, Chew W, Sornaraj P, et al.** 2016. The homeodomain transcription factor TaHDZip1-2 from wheat regulates frost tolerance, flowering time and spike development in transgenic barley. *New Phytologist* **211**, 671–687.
- Kovinich N, Kayanja G, Chanoca A, Riedl K, Otegui MS, Grotewold E.** 2014. Not all anthocyanins are born equal: distinct patterns induced by stress in Arabidopsis. *Planta* **240**, 931–940.
- Kubo H, Kishi M, Goto K.** 2008. Expression analysis of ANTHOCYANINLESS2 gene in Arabidopsis. *Plant Science* **175**, 853–857.
- Kubo H, Peeters AJ, Aarts MG, Pereira A, Koornneef M.** 1999. ANTHOCYANINLESS2, a homeobox gene affecting anthocyanin distribution and root development in Arabidopsis. *The Plant Cell* **11**, 1217–1226.
- Łata B, Trampczynska A, Paczesna J.** 2009. Cultivar variation in apple peel and whole fruit phenolic composition. *Scientia Horticulturae* **121**, 176–181.
- Li T, Jiang Z, Zhang L, Tan D, Wei Y, Yuan H, Li T, Wang A.** 2016. Apple (*Malus domestica*) MdERF2 negatively affects ethylene biosynthesis during fruit ripening by suppressing MdACS1 transcription. *The Plant Journal* **88**, 735–748.
- Li W, Wang B, Wang M, et al.** 2014. Cloning and characterization of a potato StAN1 1 gene involved in anthocyanin biosynthesis regulation. *Journal of Integrative Plant Biology* **56**, 364–372.
- Li XL.** 2014. Mechanisms of the signal transduction for ethylene production in apple (*Malus domestica*) fruit development and ripening. PhD thesis, China Agricultural University.
- Li YY, Mao K, Zhao C, Zhao XY, Zhang HL, Shu HR, Hao YJ.** 2012. MdCOP1 ubiquitin E3 ligases interact with MdMYB1 to regulate light-induced anthocyanin biosynthesis and red fruit coloration in apple. *Plant Physiology* **160**, 1011–1022.
- Lin Z, Hong Y, Yin M, Li C, Zhang K, Grierson D.** 2008. A tomato HD-Zip homeobox protein, LeHB-1, plays an important role in floral organogenesis and ripening. *The Plant Journal* **55**, 301–310.
- Lister CE, Lancaster JE, Sutton KH, Walker JRL.** 1997. Aglycone and glycoside specificity of apple skin flavonoid glycosyltransferase. *Journal of the Science of Food and Agriculture* **75**, 378–382.
- Liu YL, Jiang YH, Wang HJ, Qi YW, Liu CH, Ren XL.** 2015. Self-activation and interaction protein analysis of MdHB1 transcription factor in apple. *Plant Physiology Journal* **51**, 5.
- Lou Q, Liu Y, Qi Y, Jiao S, Tian F, Jiang L, Wang Y.** 2014. Transcriptome sequencing and metabolite analysis reveals the role of delphinidin metabolism in flower colour in grape hyacinth. *Journal of Experimental Botany* **65**, 3157–3164.
- Lü P, Zhang C, Liu J, et al.** 2014. RhHB1 mediates the antagonism of gibberellins to ABA and ethylene during rose (*Rosa hybrida*) petal senescence. *The Plant Journal* **78**, 578–590.
- Matsumoto T, Morishige H, Tanaka T, Kanamori H, Komatsuda T, Sato K, Itoh T, Wu J, Nakamura S.** 2014. Transcriptome analysis of barley identifies heat shock and HD-Zip I transcription factors up-regulated in response to multiple abiotic stresses. *Molecular Breeding* **34**, 761–768.
- Medina-Puche L, Cumplido-Laso G, Amil-Ruiz F, et al.** 2014. MYB10 plays a major role in the regulation of flavonoid/phenylpropanoid metabolism during ripening of *Fragaria×ananassa* fruits. *Journal of Experimental Botany* **65**, 401–417.
- Montefiori M, Brendolise C, Dare AP, Lin-Wang K, Davies KM, Hellens RP, Allan AC.** 2015. In the Solanaceae, a hierarchy of bHLHs confer distinct target specificity to the anthocyanin regulatory complex. *Journal of Experimental Botany* **66**, 1427–1436.
- Morker KH, Roberts MR.** 2011. Light exerts multiple levels of influence on the Arabidopsis wound response. *Plant, Cell and Environment* **34**, 717–728.
- Morohashi K, Zhao M, Yang M, Read B, Lloyd A, Lamb R, Grotewold E.** 2007. Participation of the Arabidopsis bHLH factor GL3 in trichome initiation regulatory events. *Plant Physiology* **145**, 736–746.
- Papadopoulos DK, Skouloudaki K, Adachi Y, Samakovlis C, Gehring WJ.** 2012. Dimer formation via the homeodomain is required for function and specificity of Sex combs reduced in Drosophila. *Developmental Biology* **367**, 78–89.
- Pattanaik S, Kong Q, Zaitlin D, Werkman JR, Xie CH, Patra B, Yuan L.** 2010. Isolation and functional characterization of a floral tissue-specific R2R3 MYB regulator from tobacco. *Planta* **231**, 1061–1076.
- Petroni K, Tonelli C.** 2011. Recent advances on the regulation of anthocyanin synthesis in reproductive organs. *Plant Science* **181**, 219–229.
- Ré DA, Capella M, Bonaventure G, Chan RL.** 2014. Arabidopsis AtHB7 and AtHB12 evolved divergently to fine tune processes associated with growth and responses to water stress. *BMC Plant Biology* **14**, 150.
- Rice EA, Khandelwal A, Creelman RA, et al.** 2014. Expression of a truncated ATHB17 protein in maize increases ear weight at silking. *PLoS One* **9**, e94238.
- Romani F, Ribone PA, Capella M, Miguel VN, Chan RL.** 2016. A matter of quantity: Common features in the drought response of transgenic plants overexpressing HD-Zip I transcription factors. *Plant Science* **251**, 139–154.
- Saleh A, Lumberras V, Lopez C, Dominguez-Puigjaner E, Kizis D, Pagès M.** 2006. Maize DBF1-interactor protein 1 containing an R3H domain is a potential regulator of DBF1 activity in stress responses. *The Plant Journal* **46**, 747–757.
- Schaart JG, Dubos C, Romero De La Fuente I, et al.** 2013. Identification and characterization of MYB–bHLH–WD40 regulatory complexes controlling proanthocyanidin biosynthesis in strawberry (*Fragaria × ananassa*) fruits. *New Phytologist* **197**, 454–467.
- Sessa G, Morelli G, Ruberti I.** 1993. The Athb-1 and -2 HD-Zip domains homodimerize forming complexes of different DNA binding specificities. *EMBO Journal* **12**, 3507–3517.
- Song A, Li P, Xin J, Chen S, Zhao K, Wu D, Fan Q, Gao T, Chen F, Guan Z.** 2016. Transcriptome-wide survey and expression profile analysis of putative chrysanthemum HD-Zip I and II genes. *Genes* **7**, 19.
- Sun D, Nandety RS, Zhang Y, Reid MS, Niu L, Jiang CZ.** 2016. A petunia ethylene-responsive element binding factor, PhERF2, plays an important role in antiviral RNA silencing. *Journal of Experimental Botany* **67**, 3353–3365.
- Sun RZ, Pan QH, Duan CQ, Wang J.** 2015. Light response and potential interacting proteins of a grape flavonoid 3'-hydroxylase gene promoter. *Plant Physiology and Biochemistry* **97**, 70–81.
- Sunilkumar G, Vijayachandra K, Veluthambi K.** 1999. Preincubation of cut tobacco leaf explants promotes Agrobacterium-mediated transformation by increasing vir gene induction. *Plant Science* **141**, 51–58.
- Sun-Waterhouse D, Luberriaga C, Jin D, Wibisono R, Wadhwa SS, Waterhouse GIN.** 2013. Juices, fibres and skin waste extracts from white, pink or red-fleshed apple genotypes as potential food ingredients. *Food and Bioprocess Technology* **6**, 377–390.
- Takos AM, Jaffé FW, Jacob SR, Bogs J, Robinson SP, Walker AR.** 2006a. Light-induced expression of a MYB gene regulates anthocyanin biosynthesis in red apples. *Plant Physiology* **142**, 1216–1232.
- Takos AM, Ubi BE, Robinson SP, Walker AR.** 2006b. Condensed tannin biosynthesis genes are regulated separately from other flavonoid biosynthesis genes in apple fruit skin. *Plant Science* **170**, 487–499.
- Tian Z, He Q, Wang H, Liu Y, Zhang Y, Shao F, Xie C.** 2015. The potato ERF transcription factor StERF3 negatively regulates resistance to *Phytophthora infestans* and salt tolerance in potato. *Plant and Cell Physiology* **56**, 992–1005.
- Wang P, Du Y, Zhao X, Miao Y, Song CP.** 2013. The MPK6-ERF6-ROS-responsive cis-acting Element7/GCC box complex modulates oxidative gene transcription and the oxidative response in Arabidopsis. *Plant Physiology* **161**, 1392–1408.

- Wang X, Wei Z, Ma F.** 2015. The effects of fruit bagging on levels of phenolic compounds and expression by anthocyanin biosynthetic and regulatory genes in red-fleshed apples. *Process Biochemistry* **50**, 1774–1782.
- Wang YJ, Li YD, Luo GZ, Tian AG, Wang HW, Zhang JS, Chen SY.** 2005. Cloning and characterization of an HDZip I gene GmHZ1 from soybean. *Planta* **221**, 831–843.
- Wang Z, Meng D, Wang A, Li T, Jiang S, Cong P, Li T.** 2013. The methylation of the PcMYB10 promoter is associated with green-skinned sport in Max Red Bartlett pear. *Plant Physiology* **162**, 885–896.
- Wen XH, Jiang YH, Zhou K, Ren XL.** 2015. Effects of virus-induced *MdHB-1* silencing on apple fruit ripening. *Acta Agriculturae Boreali-Occidentalis Sinica* **24**, 113–119.
- Wolfe KL, Liu RH.** 2003. Apple peels as a value-added food ingredient. *Journal of Agricultural and Food Chemistry* **51**, 1676–1683.
- Wu R, Wang T, McGie T, Voogd C, Allan AC, Hellens RP, Varkonyi-Gasic E.** 2014. Overexpression of the kiwifruit *SVP3* gene affects reproductive development and suppresses anthocyanin biosynthesis in petals, but has no effect on vegetative growth, dormancy, or flowering time. *Journal of Experimental Botany* **65**, 4985–4995.
- Xie XB, Li S, Zhang RF, et al.** 2012. The bHLH transcription factor MdbHLH3 promotes anthocyanin accumulation and fruit colouration in response to low temperature in apples. *Plant, Cell and Environment* **35**, 1884–1897.
- Xu W, Grain D, Bobet S, Le Gourrierrec J, Thévenin J, Kelemen Z, Lepiniec L, Dubos C.** 2014. Complexity and robustness of the flavonoid transcriptional regulatory network revealed by comprehensive analyses of MYB–bHLH–WDR complexes and their targets in Arabidopsis seed. *New Phytologist* **202**, 132–144.
- Yu Y, Xu W, Wang J, et al.** 2013. The Chinese wild grapevine (*Vitis pseudoreticulata*) E3 ubiquitin ligase Erysiphe necator-induced RING finger protein 1 (EIRP1) activates plant defense responses by inducing proteolysis of the VpWRKY11 transcription factor. *New Phytologist* **200**, 834–846.
- Zhai R, Wang Z, Zhang S, Meng G, Song L, Wang Z, Li P, Ma F, Xu L.** 2016. Two MYB transcription factors regulate flavonoid biosynthesis in pear fruit (*Pyrus bretschneideri* Rehd.). *Journal of Experimental Botany* **67**, 1275–1284.
- Zhang F, Zuo K, Zhang J, Liu X, Zhang L, Sun X, Tang K.** 2010. An L1 box binding protein, GbML1, interacts with GbMYB25 to control cotton fibre development. *Journal of Experimental Botany* **61**, 3599–3613.
- Zhang XJ, Wang LX, Liu YL, Chen XX, Yang YZ, Zhao ZY.** 2013. Differential gene expression analysis of 'Granny Smith' apple (*Malus domestica* Borkh.) during fruit skin coloration. *South African Journal of Botany* **88**, 125–131.
- Zhao M, Morohashi K, Hatlestad G, Grotewold E, Lloyd A.** 2008. The TTG1–bHLH–MYB complex controls trichome cell fate and patterning through direct targeting of regulatory loci. *Development* **135**, 1991–1999.
- Zhao Y, Ma Q, Jin X, et al.** 2014. A novel maize homeodomain-leucine zipper (HD-Zip) I gene, *Zmhdz10*, positively regulates drought and salt tolerance in both rice and Arabidopsis. *Plant and Cell Physiology* **55**, 1142–1156.
- Zhou H, Lin-Wang K, Wang H, Gu C, Dare AP, Espley RV, He H, Allan AC, Han Y.** 2015. Molecular genetics of blood-fleshed peach reveals activation of anthocyanin biosynthesis by NAC transcription factors. *The Plant Journal* **82**, 105–121.